Simulation-driven parameter study of concentric Halbach cylinders for magnetorheological robotic grasping

Non Peer-reviewed author version

CRAMER, Jeroen; CRAMER, Martijn; DEMEESTER, Eric & KELLENS, Karel (2022) Simulation-driven parameter study of concentric Halbach cylinders for magnetorheological robotic grasping. In: JOURNAL OF MAGNETISM AND MAGNETIC MATERIALS, 546 (Art N° 168637).

DOI: 10.1016/j.jmmm.2021.168637
Handle: http://hdl.handle.net/1942/37285

Simulation-driven parameter study of concentric Halbach cylinders for magnetorheological robotic grasping

Jeroen Cramer[a,*], Martijn Cramer[a], Eric Demeester[a], Karel Kellens[a]

[a] *KU Leuven, Diepenbeek Campus, Dept. of Mechanical Engineering, Research unit ACRO, B-3000 Leuven, Belgium*

Abstract

Due to their peculiar property of controlled stiffness and strength under an external magnetic field, magnetorheological (MR) fluids show great potential in developing hybrid robotic grippers that in the future could offer the same versatility as the human hand. This demands for sufficiently strong, compact and switchable magnetic field sources for which permanent magnets are often overshadowed by electromagnets. However, permanent magnets possess higher magnetic flux densities per mass unit, and when assembled in certain ways, they allow to control their joint magnetic field. Within this paper, an extensive parameter study is conducted using grid search for the design of concentric Halbach cylinder assemblies based on finite element simulations. The influence of decisive geometric and material properties on the performance of these magnetic activation mechanisms is studied. These include the magnets' shapes, sizes and number; the cylinders' radii and number of pole pairs; and the relative permeabilities of the MR fluid and the grasped object. The performance of a design is measured by a multi-objective function that considers: the mean magnetic flux densities generated in the mechanism's ON and OFF-state, the magnetic field's inhomogeneity (i.e. standard deviation) in the ON-state, and the total magnet area for both cylinders. This work concludes by deriving guidelines for the most optimal design of concentric Halbach cylinders for a cylindrical radial bellow gripper.

Keywords: Permanent magnet assemblies, Halbach cylinder, Magnetorheological fluid, Robotic grasping

1. Introduction

Nowadays, one becomes aware of the growing uncertain (e.g. advanced random bin picking) and dynamic (e.g. human-robot collaboration) environments in manufacturing industry and tries to enhance the functionalities of conventional industrial grippers, based on force and form closure, by implementing soft deformable structures [1]. Soft grasping can be categorised into three principles: grasping (1) by controlled actuation, (2) by controlled adhesion and (3) by controlled stiffness [2]. Grasping by stiffness consists of enveloping the target object softly, and subsequently stiffening the structure to secure the grasped object; it is divided into: granular jamming [3], low-melting point alloys (LMPA) [4], and electrorheological (ER) and magnetorheological (MR) fluids [5].

In the presence of respectively an electric or magnetic field, ER and MR fluids reversibly change in aggregation state from free-flowing liquids (i.e. Newtonian fluid) to viscoelastic solids (i.e. Bingham plastic) within milliseconds [5]. Based on an exhaustive comparison of the mechanical and electrical properties of both ER and MR fluids presented in [5], MR fluids have been selected to facilitate hybrid gripper applications [6]. MR fluids are composed of micron-sized magnetically permeable particles suspended in a non-magnetic carrier medium, typically carbonyl iron (CI) particles in a mineral or silicone oil [5, 7]. Its mechanical strength is attributed to the alignment of these particles into the formation of linear chains parallel to the magnetic field lines. After withdrawal of the magnetic field, the MR fluid regains its original aggregation state. The stiffness and the corresponding yield stress of the MR fluid can be adjusted by varying the magnitude of the applied magnetic field. Although great potential of magnetorheological materials has been demonstrated in various applications [8, 9, 10, 11, 12], the applications in robotics and grippers remain limited due to a number of pending challenges [6]. In order to enter the commercial market, industry imposes three main requirements to MR hybrid grippers, namely: higher grasping forces, higher grasping speeds and more compact devices [6]. Therefore,

*Corresponding author: jeroen.cramer@kuleuven.be

necessary research tracks are: optimising the rheological, electromagnetic and mechanical properties of MR fluids, as well as improving the mechatronic design of MR hybrid devices [6]. This work offers an answer to the latter by deriving guidelines for the most optimal design of a circular permanent magnet assembly (i.e. Halbach cylinder) to activate the MR fluid, as force transferring medium, in a robotic gripper prototype.

In order to use permanent magnet assemblies for grasping, the magnetic field should be adjustable to establish and release the grasp while limiting the magnetic field outside the gripper. Electromagnets are often considered as the sole option in obtaining controllable magnetic flux densities. But, vast number of turns or large wire cross sections are necessary to yield similar magnetic flux densities compared to permanent magnets. In addition, at these flux densities, electromagnets have to be actively cooled due to high electric currents. By combining common single permanent magnet assemblies, adjustable magnetic field sources can be created (e.g [13, 14]). Bjørk et al. [14] simulated five different designs, and concluded that two concentric Halbach cylinders generate the highest magnetic flux density in the cylinder's core for the least amount of magnetic material. The magnetic field is controlled by applying a relative angular rotation between the two Halbach cylinders (Fig. 1). Furthermore, this design has the advantages of a nearly homogeneous magnetic field, the need of little to no actuation forces [15], and its compactness compared with other permanent magnet assemblies since regulating the magnetic field's magnitude does not increase its external dimensions or shape. Halbach cylinders have already proven their usefulness in various applications, for instance in magnetic refrigeration devices [16], nuclear magnetic resonance (NMR) apparatus [17, 18] and a permanent magnet system to guide superparamagnetic nanoparticles on arbitrary trajectories [19].

This work is organised as follows. Section 2 presents the developed cylindrical radial bellow gripper. Section 3 describes the geometric structures of the finite element meshes of both annular and square segmented Halbach cylinders. Section 4 validates the numerical model and solver against the well-established Halbach formula, and formulates the proposed multi-objective function. In Section 5, an extensive parameter study is conducted using grid search from which guidelines are drawn for the design of magnetic activation mechanisms for the developed robotic gripper. Section 6 discusses the results of current research and points to future research tracks. Finally, Section 7 concludes with a brief summary of this work.

2. Stiffness-adaptable robotic gripper prototype

In the authors' opinion, the application of concentric Halbach cylinders in the field of robotic grasping is twofold: (1) as astrictive magnetic grippers analogous to conventional electromagnets, or (2) in combination with stiffness-adaptable materials for soft grasping [6].

This research presents a cylindrical radial bellow gripper filled with MR fluid (Fig. 2). The rubber membrane inside the gripper's hollow core is actuated by pressurising the MR fluid in its liquid state via the fluid inlet, forming four symmetrical bellows that inflate radially towards the centre. The core and membrane are dimensioned such that axial objects (e.g. stepped transmission shafts) with diameters ranging from 10 to 58 mm can be grasped, according to Zimmer's RG10-60 compressed air variant[1]. Compared to air as force-transferring medium, MR fluid could improve the pull and bending stiffness of the radial bellows in vertical and horizontal object positions, respectively. Pressurising the MR fluid before magnetisation could even increase its yield stress by a factor of 10 [20]. A magnetic activation mechanism of two concentric Halbach cylinders, guided by two axial bearings, is placed on the outer circumference of the gripper's housing. A worm drive provides the relative angular rotation of the Halbach cylinders to switch the magnetic field inside the gripper's core on (and off), changing the MR fluid's aggregation state to obtain (and release) a secure grasp. The worm wheel is attached to the movable outer cylinder while the inner cylinder is fixed in the gripper's housing. Compared to regular spur gears, the worm drive (1) is considerably smaller; (2) transmits higher torques due to its high reduction ratios in one stage; and (3) eliminates the backdrivability of the outer cylinder (i.e. self-locking) caused by intramagnetic forces during rotation.

In theory, Halbach cylinders are often represented as infinitely long, one-piece magnet annuli in which the magnetisation direction varies continuously. However in practice, magnet annuli have finite lengths [21] and have to be constructed from individual segments whose direction of magnetisation varies in a discrete manner. First, both Halbach cylinders are foreseen along the entire length (45 mm) of the radial bellows: to homogeneously stiffen the MR fluid in axial direction within the bellows, and to deal with adverse effects at the cylinders' end faces related with large radius to length ratios

[1] https://www.zimmer-group.com/en/technologies-components/components/handling-technology/grippers/pneumatic/grippers-for-special-tasks/series-rg/products/rg10-60

of Halbach cylinders. Second, segmentation of the magnet annuli causes a decrease in the theoretically achievable magnetic flux density, generated in the gripper's core. In contrast, this research differs by shaping the magnet annuli with square segments instead of annular segments, first proposed by [22]. In order to keep these square segments in place, a non-ferromagnetic cage has to be manufactured for both cylinders at which the magnetic flux density in the gripper's core will reduce compared to homogeneously stacked annular segments. On the other hand, square segments will improve the economic affordability, due to its standard purchasable shape, since machining magnets entails an increased cost.

To compare individual Halbach cylinders with different inner and outer radii, a dimensionless area fraction Λ of the cylinder's magnet to core area is derived (Eq. 1). In literature, Halbach cylinders are investigated for static applications where dimensions and mass are of minor importance, so large area fractions are prevalent. However, in dynamic applications (e.g. robotic grasping) dimensions and mass are crucial, as they affect dynamic forces and moments of inertia, so small area fractions are recommended. This will in turn positively affect the economic affordability in commercial applications, due to the lower amount of magnetic material.

$$\Lambda := \begin{cases} \dfrac{\left(r_o^2 - r_i^2\right)\pi}{r_i^2 \pi} & \text{annular segments} \\ \dfrac{na^2}{r_i^2 \pi} & \text{square segments} \end{cases} \tag{1}$$

where r_o is the Halbach cylinder's outer radius, r_i is the Halbach cylinder's inner radius, n is the number of square magnet segments, and a is the side length of square magnet segments. The total area fraction of two concentric Halbach cylinders ${}^1\Lambda$ is calculated by combining the area fractions of the inner and outer cylinders ${}^2\Lambda_{in}$ and ${}^2\Lambda_{out}$ (Eq. 2):

$${}^1\Lambda := {}^2\Lambda_{in} + {}^2\Lambda_{in}{}^2\Lambda_{out} + {}^2\Lambda_{out} \tag{2}$$

Eq. 2 allows to construct two concentric Halbach cylinders with the same overall magnetic volume and output comparable to a single Halbach cylinder but with the possibility to switch the magnetic field in the cylinder's core on and off. As will be motivated in Section 4, three characteristic area fractions ${}^1\Lambda$ of 0.25, 0.5, 1.0 are studied.

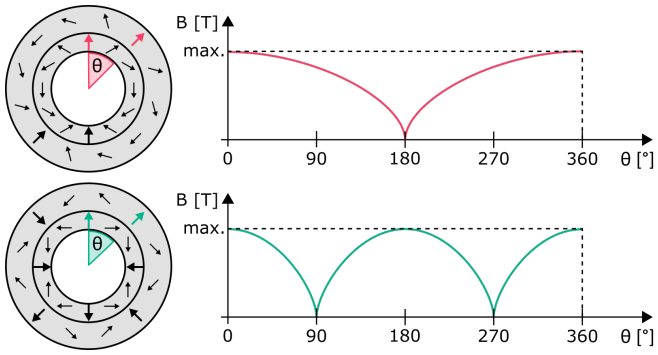

Figure 1: Illustration of two concentric Halbach cylinders' function with one pole pair or dipole (red, top), and two pole pairs or quadrupole (green, bottom). The magnetic flux density is adjusted by applying a relative angular rotation θ between the two Halbach cylinders, represented by the coloured core areas. Note that in practice the maximum magnetic flux densities are not necessarily the same for both magnet configurations as shown in this figure.

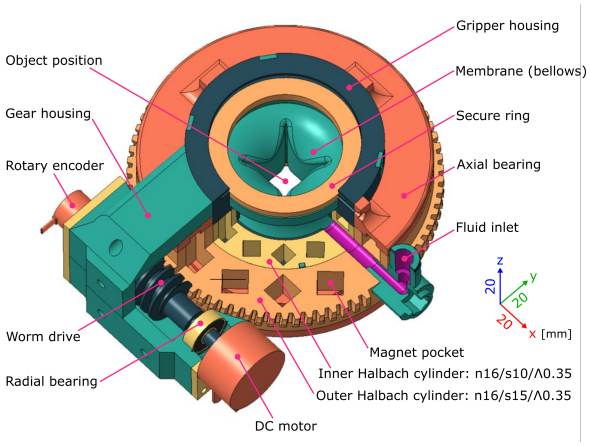

Figure 2: Local cross section of the developed gripper prototype consisting of a membrane inflated with MR fluid, forming four radial bellows, and magnetically activated by two concentric Halbach cylinders, which are optimised by the parameter study in this research (n: number of square magnets, s: magnets' side length [mm], and Λ: dimensionless area fraction).

3. Halbach cylinder's mesh construction

This section describes the geometric structures of the individual Halbach cylinder's meshes for the two-dimensional magnetostatic analyses conducted in Section 5.

3.1. Halbach cylinder with annular segments

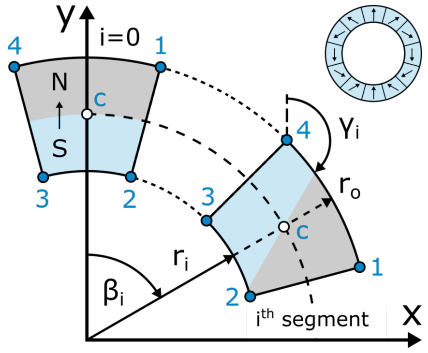

Figure 3: Illustration of the annular segment's pose, determined by Eq. 3. r_i is the cylinder's inner radius, r_o is the cylinder's outer radius, β_i is the position angle of the i$^{\text{th}}$ segment in the Halbach cylinder and the magnetisation direction γ_i of each magnet segment is also given by Eq. 4.

The four vertices of each annular magnet segment are described by the position vectors in Eq. 3, corresponding to Fig. 3, which are necessary to construct their finite element meshes.

$$
\begin{aligned}
{}^1\vec{p}_i &:= \begin{pmatrix} {}^1x_i \\ {}^1y_i \end{pmatrix} = r_o \begin{pmatrix} \sin(\beta_i + \frac{\alpha}{2}) \\ \cos(\beta_i + \frac{\alpha}{2}) \end{pmatrix} \\
{}^2\vec{p}_i &:= \begin{pmatrix} {}^2x_i \\ {}^2y_i \end{pmatrix} = r_i \begin{pmatrix} \sin(\beta_i + \frac{\alpha}{2}) \\ \cos(\beta_i + \frac{\alpha}{2}) \end{pmatrix} \\
{}^3\vec{p}_i &:= \begin{pmatrix} {}^3x_i \\ {}^3y_i \end{pmatrix} = r_i \begin{pmatrix} \sin(\beta_i - \frac{\alpha}{2}) \\ \cos(\beta_i - \frac{\alpha}{2}) \end{pmatrix} \\
{}^4\vec{p}_i &:= \begin{pmatrix} {}^4x_i \\ {}^4y_i \end{pmatrix} = r_o \begin{pmatrix} \sin(\beta_i - \frac{\alpha}{2}) \\ \cos(\beta_i - \frac{\alpha}{2}) \end{pmatrix} \\
\beta_i &:= i\alpha \quad \text{for i = 0, 1,..., n-1} \\
\alpha &:= \frac{2\pi}{n}
\end{aligned}
\tag{3}
$$

where ${}^j\vec{p}_i$ is the position vector of the j$^{\text{th}}$ vertex, ${}^jx_i$ and ${}^jy_i$ are the Cartesian coordinates of the j$^{\text{th}}$ vertex, r_i is the cylinder's inner radius, r_o is the cylinder's outer radius, n is the number of annular magnet segments, β_i is the position angle of the i$^{\text{th}}$ segment in the Halbach cylinder. The magnetisation direction of each magnet segment is given by Eq. 4, that allows to approximate the magnetisation in a continuous Halbach cylinder.

$$\gamma_i := (1 + k)\beta_i \text{ with } k \in \mathbb{Z} \text{ and } i = 0, 1, \ldots, n-1 \tag{4}$$

where γ_i is the magnetisation direction of the i$^{\text{th}}$ segment, k is the number of pole pairs with positive and negative values for internal and external magnetic fields respectively.

3.2. Halbach cylinder with square segments

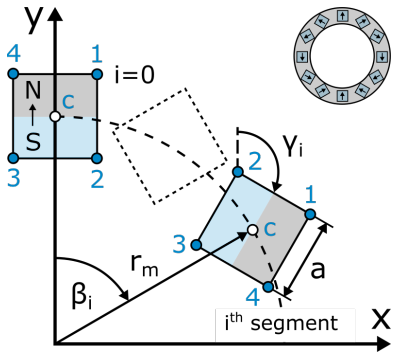

Figure 4: Illustration of the square segment's pose, determined by Eq. 5. Where r_m is the magnets' centre radius, a is the magnet segment's side length, β_i is the position angle of the i$^{\text{th}}$ segment in the Halbach cylinder and the magnetisation direction γ_i of each magnet segment is also given by Eq. 4. Adapted from [22].

The four vertices of each square magnet segment are described by the position vectors in Eq. 5, established by Raich et al. [22] and corresponding to Fig. 4, which are necessary to construct their finite element meshes.

$$
\begin{aligned}
{}^1\vec{p}_i &:= \begin{pmatrix} {}^1x_i \\ {}^1y_i \end{pmatrix} = r_m \begin{pmatrix} \sin\beta_i \\ \cos\beta_i \end{pmatrix} + \frac{a}{\sqrt{2}} \begin{pmatrix} \cos\zeta_i \\ \sin\zeta_i \end{pmatrix} \\
{}^2\vec{p}_i &:= \begin{pmatrix} {}^2x_i \\ {}^2y_i \end{pmatrix} = r_m \begin{pmatrix} \sin\beta_i \\ \cos\beta_i \end{pmatrix} + \frac{a}{\sqrt{2}} \begin{pmatrix} -\sin\zeta_i \\ \cos\zeta_i \end{pmatrix} \\
{}^3\vec{p}_i &:= \begin{pmatrix} {}^3x_i \\ {}^3y_i \end{pmatrix} = r_m \begin{pmatrix} \sin\beta_i \\ \cos\beta_i \end{pmatrix} + \frac{a}{\sqrt{2}} \begin{pmatrix} -\cos\zeta_i \\ -\sin\zeta_i \end{pmatrix} \\
{}^4\vec{p}_i &:= \begin{pmatrix} {}^4x_i \\ {}^4y_i \end{pmatrix} = r_m \begin{pmatrix} \sin\beta_i \\ \cos\beta_i \end{pmatrix} + \frac{a}{\sqrt{2}} \begin{pmatrix} \sin\zeta_i \\ -\cos\zeta_i \end{pmatrix} \\
\beta_i &:= i\alpha \quad \text{for i = 0, 1,..., n-1} \\
\alpha &:= \frac{2\pi}{n} \\
\zeta_i &:= \frac{\pi}{4} - \gamma_i
\end{aligned}
\tag{5}
$$

where ${}^{j}\vec{p}_i$ is the position vector of the j$^{\text{th}}$ vertex, ${}^{j}x_i$ and ${}^{j}y_i$ are the Cartesian coordinates of the j$^{\text{th}}$ vertex, r_m is the magnets' centre radius, a is the magnet segment's side length, n is the number of square magnet segments, β_i is the position angle of the i$^{\text{th}}$ segment in the Halbach cylinder and the magnetisation direction γ_i of each magnet segment is also given by Eq. 4, that allows to approximate the magnetisation in a continuous Halbach cylinder.

In case of Halbach cylinders with annular segments, the magnets' centre radius is defined as the average of the inner and outer radii, and is independent of the number of magnet segments. This is in contrast to Halbach cylinders with square segments of which the magnets' centre radius does depend on the number of magnets. Fig. 5 demonstrates the use of both formulas in Eq. 6 to determine the magnets' centre radius r_m, where r_v is the radius of the circle formed by the inward-pointing vertices of the annular stacked square magnets, r_i is the Halbach cylinder's inner radius, n is the number of square segments, d and a respectively stand for a square magnet's diagonal and side length, and χ is an arbitrary chosen factor, set to 1.05, to prevent the intersection of the magnets' finite element meshes.

$$
\begin{aligned}
r_m &:= \left(r_i + \frac{d}{2}\right)\chi \qquad \text{for: } r_v < r_i \\
r_m &:= \frac{d}{2}\csc\left(\frac{\alpha}{2}\right)\chi \qquad \text{for: } r_v \geq r_i
\end{aligned}
\tag{6}
$$

With:

$$
\begin{aligned}
d &:= \sqrt{2}a \\
\chi &\geq 1 \\
\alpha &:= \frac{2\pi}{n} \\
r_v &:= \frac{a}{\sqrt{2}}\left[\csc\left(\frac{\alpha}{2}\right) - 1\right]
\end{aligned}
$$

In order to make Eq. 6 generally applicable, regardless of dipoles or quadrupoles, worst case magnet stacking is assumed for which all magnets have their diagonals radially and tangentially oriented (Fig. 5). They therewith occupy the largest space in their cage. In the first scenario at for instance 4 magnets, the tangentially oriented diagonals lead to a cubic stacking of which r_v is less than r_i (Fig. 5 - left, faded segments). To force the 4 magnets inside their annular cage (Fig. 5 - left, dark segments), the first formula is designed. In the second scenario at for instance 24 magnets, r_v is greater than r_i (Fig. 5 - right). This allows the use of the second formula, which describes the radius of the enclosing circle of the polygon formed by the tangentially oriented diagonals. Both formulas translate into two trends pictured in Fig. 6, independent of the cylinder's inner radius. In general, it can be stated that Halbach cylinders with square segments have larger cross-sectional dimensions than those with annular segments, which is even more noticeable at higher area fractions as the number of magnet segments increases.

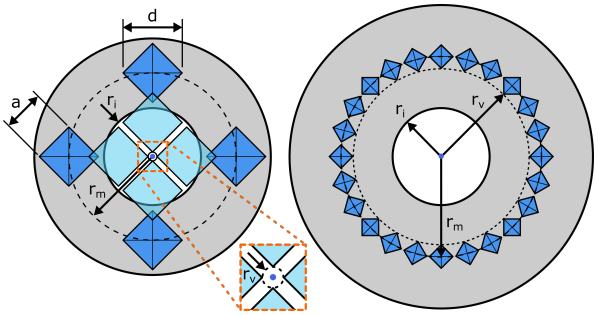

Figure 5: Illustration of the magnets' centre radius r_m (left: $r_v < r_i$; right: $r_v \geq r_i$) for a square segmented Halbach cylinder (with an area fraction Λ of 1.0).

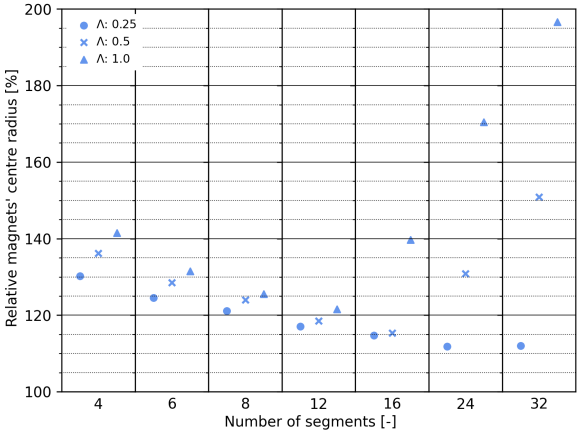

Figure 6: Relative magnets' centre radius [%] of a square segmented Halbach cylinder relative to an annular segmented Halbach cylinder, as a function of the number of magnet segments, the area fraction Λ (marker symbols) and independent of the cylinder's inner radius. Even numbers of magnet segments were studied, with the spread per number of magnet segments for better visibility.

4. Simulation and modelling framework

In this work, a Python framework is developed that automatically configures and simulates numerous two-dimensional designs of Halbach cylinders from a user-specified grid space of geometric and material parameters:

- Number of Halbach cylinders,
- Number of pole pairs (i.e. dipole or quadrupole),
- Number of magnet segments,
- Shape of magnet segments (i.e. annular or square),
- Area fraction(s) of the Halbach cylinder(s) which include(s) the inner and outer radii,
- Relative permeability of the object to be grasped,
- Relative permeability of the substance in the radial bellows,
- Relative permeability of the annular magnet cages (only applicable for square magnets),
- Relative permeability of the magnet segments.

In this paper, designs of two concentric Halbach cylinders are examined that consist of annular or square segments, of which the inner cylinder's core (i.e. radial bellows) is filled with a magnetically conductive substance. The multiphysics software *CSC Elmer*[2], its *MagnetoDynamics2D* model and built-in *UMFPack* solver, to solve sparse direct linear systems, are employed to simultaneously simulate each candidate design in its ON and OFF-state. From the resulting magnetic vector potentials, the magnetic flux densities are derived by means of Elmer's *MagnetoDynamicsCalcFields* subroutine. Results are post-processed and visualised using Kitware's Visualisation Toolkit (VTK)[3] and Matplotlib[4].

The designs' performance is characterised by a multi-objective function (Eq. 7) composed of a linear combination of the mean magnetic flux densities in the Halbach cylinders' ON and OFF-state $\bar{B}_{ON}$ and $\bar{B}_{OFF}$, the magnetic flux density's inhomogeneity in the ON-state ΔB_{ON} (i.e. standard deviation), and the total area of magnet segments in both cylinders A_m. The choice of these quantities is inspired by [22], used to optimise their design of a dipolar Halbach cylinder with identical bar magnets to use in mobile NMR/MRI devices. Since these quantities differ in term of units and orders of magnitude, a fair comparison requires normalisation (Eq. 8) where the minimum and maximum values of the complete dataset of analysed Halbach designs are employed. The magnetic flux densities represent the mean values of the two-dimensional resultants of each mesh node taken over the entire area of the radial bellows in the gripper's core. Maximising the multi-objective function will result in: (1) a strong homogeneous magnetic field in the ON-state ensuring solid grasps; (2) little to no magnetic field in the OFF-state guaranteeing a sufficiently low MR fluid viscosity to improve both the gripper's formability around the object shape during grasping as well as the release of the grasped object; and (3) minimal amount of magnetic material restricting the gripper's mass, volume, and cost. Finally, by means of the weight factors w_i, one can alter the relative importance of each quantity.

[2]https://www.csc.fi/web/elmer
[3]https://vtk.org/
[4]https://matplotlib.org/

Table 1: Percent deviation [%] of numerically to analytically determined mean magnetic flux densities in a Halbach cylinder's core, as a function of the number of annular segments shaped into a dipole. Mean μ and standard deviation σ are taken over area fractions Λ of 0.25, 0.5, and 1.0 for each number of segments. The relative magnetic permeabilities μ_r are 1.0 for the magnet segments and core material, as stated by the Halbach formula's prerequisites. The remanence B_{rem} is 1.4 T, which is typical for NdFeB magnets.

n	4	6	8	12	16	24	32
$\boldsymbol{\mu}$ [%]	6.97	4.30	2.84	1.26	0.66	0.22	0.13
$\boldsymbol{\sigma}$ [%]	2.46	1.81	1.48	0.75	0.45	0.17	0.09

$$O = w_1\langle\bar{B}_{ON}\rangle + w_2\langle\bar{B}_{OFF}\rangle + w_3\langle\Delta B_{ON}\rangle + w_4\langle A_m\rangle \tag{7}$$

With:

$$\begin{aligned}
\langle\bar{B}_{ON}\rangle &:= \frac{\bar{B}_{ON} - min\{\bar{B}_{ON}\}}{max\{\bar{B}_{ON}\} - min\{\bar{B}_{ON}\}} \\
\langle\bar{B}_{OFF}\rangle &:= \frac{max\{\bar{B}_{OFF}\} - \bar{B}_{OFF}}{max\{\bar{B}_{OFF}\} - min\{\bar{B}_{OFF}\}} \\
\langle\Delta B_{ON}\rangle &:= \frac{max\{\Delta B_{ON}\} - \Delta B_{ON}}{max\{\Delta B_{ON}\} - min\{\Delta B_{ON}\}} \\
\langle A_m\rangle &:= \frac{max\{A_m\} - A_m}{max\{A_m\} - min\{A_m\}}
\end{aligned} \tag{8}$$

The numerical model and solver are validated against the well-established Halbach formula (Eq. 9) [23]. The mean magnetic flux density $\bar{B}_c$ inside a single two-dimensional Halbach annulus' core with one pole pair (i.e. dipole) is analytically determined by Eq. 9. The following values for the equation quantities are used:

(1) relative magnetic permeabilities of 1.0 for the magnet segments and core material, as stated by the Halbach formula's prerequisites; (2) a remanence B_{rem} of 1.4 T which is typical for NdFeB magnets: the most widely used permanent magnet alloy in engineering applications; (3) area fractions Λ of 0.25, 0.5, 1.0 that are recommended by the authors for dynamic robotic applications taking into account the gripper's weight, compactness and economic affordability; and (4) an increasing number of annular segments.

$$\begin{aligned}\bar{B}_c &:= B_{rem} \ln\left(\frac{r_o}{r_i}\right)\eta \\ &= B_{rem} \ln\left(\sqrt{\Lambda + 1}\right)\eta\end{aligned} \tag{9}$$

With:

$$\Lambda := \frac{\left(r_o^2 - r_i^2\right)\pi}{r_i^2\pi} = \left(\frac{r_o}{r_i}\right)^2 - 1$$

$$\eta := \begin{cases} 1 & \text{continuous} \\ \dfrac{\sin\alpha}{\alpha} & \text{segmented} \end{cases}$$

$$\alpha := \frac{2\pi}{n}$$

where B_{rem} is the remanence of the magnet material, the area fraction Λ is calculated using Eq. 1 for annular segments, and η accounts for segmentation in n annular segments. Table 1 demonstrates that the numerically obtained data match the analytically obtained data, especially at increasing numbers of annular segments, which serves as a validation of the numerical model and solver.

5. Simulation-driven parameter study

In this section, an extensive parameter study is conducted using grid search from which guidelines are drawn for the design of magnetic activation mechanisms (i.e. two concentric Halbach cylinders) for the proposed robotic gripper application. Designs are compared by their performance as represented by the multi-objective function's output (Eq. 7).

The objective function's weight factors are set to $w_1 := \frac{4}{11}$, $w_2 := \frac{4}{11}$, $w_3 := \frac{1}{11}$, $w_4 := \frac{2}{11}$, by which the multi-objective value ranges between 0 and 1. Proper magnetic operation of compact Halbach mechanisms is preferred over homogeneous magnetic fields. In fact, sufficiently low magnetic flux densities in the OFF-state are essential in reversing the MR fluid's aggregation state from a viscoelastic solid back to a free-flowing liquid when deactivating the robotic gripper's magnetic activation mechanism. Sufficiently high magnetic flux densities in the ON-state are required to improve the MR fluid's yield stress and the resulting pull and bending stiffness of the gripper's radial bellows in vertical and horizontal object positions, respectively. Although, the demand for high magnetic flux densities is limited from a certain point. When looking at commercially available MR fluids' characteristics[5], it can be noted that the fluid's yield stress asymptotically progresses as a function of the externally applied magnetic field strength. Consequently, further increasing the field strength (and the therewith related magnetic flux density) from the saturation point onwards will result in minor to no gain in stiffness of the activated MR fluid. Those referred commercial MR fluids, with sufficiently low dynamic viscosities to be pumped, possess saturation points around 650 mT. The authors constrained the mean magnetic flux density for the proposed MR-based application at an absolute minimum value of 250 mT in the ON-state, and an utmost maximum value of 50 mT in the OFF-state. Halbach mechanisms that do not comply with this are excluded and represented by transparent data points. Further tests should provide more details about the necessary stiffnesses to perform various manipulation tasks.

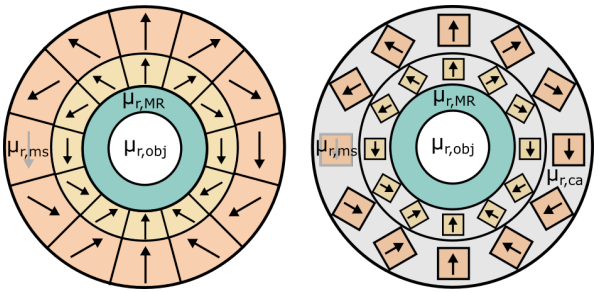

Figure 7: Illustrative representations of the Halbach mechanisms as used by the simulation and modelling framework (left: annular; right: square). The coloured areas with specific relative magnetic permeabilities represent: the grasped object (white, $\mu_{r,obj}$), the radial bellows filled with MR fluid (green, $\mu_{r,MR}$), the magnet segments of the inner cylinder (yellow, $\mu_{r,ms}$), the magnet segments of the outer cylinder (orange, $\mu_{r,ms}$), and the magnet cages (gray, $\mu_{r,ca}$).

The MR fluid's response is, in addition to the magnetic field strength, determined by the composition, weight percentage, and size of the magnetically permeable particles. An increase in these factors benefits the relative magnetic permeability as well, but adversely affects the fluid's gravitational sedimentation stability. However, many contributions were made in optimising the chemical properties of MR fluids [24]. The BH

[5] https://www.lord.com/products-and-solutions/active-vibration-control/industrial-suspension-systems/magneto-rheological-mr-fluid

curves of MR fluids are characterized by non-linearities, although single values (i.e. linear) for the relative magnetic permeability are often reported in literature: ranging from 1 to 5 [25, 26]. Similar observations were made by the authors, denoting the relative permeability range of the analyses in this section.

5.1. Halbach mechanisms with annular segments

The influence of the MR fluid's relative permeability $\mu_{r,MR}$, the radial bellows' internal grasp diameter d_g, the number of annular segments n per cylinder, and the total area fraction ${}^1\Lambda$ on the performance of several concentric Halbach cylinder designs is examined (Fig. 8 - 9):

1. In order to examine the MR fluid's relative permeability $\mu_{r,MR}$, it is assumed that the radial bellows are fully inflated, which corresponds to an internal grasp diameter d_g of 10 mm (Fig. 7, white area);
2. In order to examine the radial bellows' internal grasp diameter d_g, it is assumed that the MR fluid possess a mean relative magnetic permeability $\mu_{r,MR}$ of 2.5 (Fig. 7, green area);
3. The area fractions of the inner and outer cylinders ${}^2\Lambda_{in}$ and ${}^2\Lambda_{out}$ are the same size, generating equal magnetic flux densities to get optimal field compensations in the mechanisms' OFF-state;
4. The Halbach cylinders possess magnetic dipoles, since designs with magnetic quadrupoles completely fail to meet the flux constraints established by the authors due to the presence of stronger magnetic fields in the OFF-state. Note that a circular flux-free region, enclosed by a dense shell of magnetic field lines, is formed in the cylinder core's centre due to opposing repulsive poles when employing quadrupoles (i.e. non-homogeneous magnetic field);
5. The relative magnetic permeability of the magnet segments $\mu_{r,ms}$ is set to 1.05, which is typical for NdFeB magnets (Fig. 7, yellow and orange areas);
6. The relative magnetic permeability of the grasped object in the gripper's core $\mu_{r,obj}$ is set to 1.0 (Fig. 7, white area), which corresponds to those of commonly used non-ferromagnetic materials in engineering such as aluminum, copper, wood and plastics. No significant differences were observed with regard to the Halbach mechanisms' performance in grasping ferromagnetic objects (e.g. $\mu_{r,obj} = 1000$).

The design's performance improves:

1. at increasing relative magnetic permeabilities of the MR fluid (Fig. 8, marker colors), due to increased affinity of the magnetic field lines for the MR fluid inside the radial bellows. However, the influence of the MR fluid's relative permeability positively increases as a function of the number of magnet segments. In particular, the mean magnetic flux densities in the OFF-state become insensitive for these increasing relative permeabilities, after a certain number of magnet segments. This makes the rising mean magnetic flux densities in the ON-state more decisive. Although of minor impact, the homogeneity of the magnetic fields in the ON-state declines;
2. at increasing numbers of annular magnet segments, due to strongly decreasing mean magnetic flux densities in the OFF-state against asymptotically increasing mean magnetic flux densities in the ON-state. In addition, the homogeneity of the magnetic fields in the ON-state also enhances;
3. at increasing area fractions for large numbers of magnet segments (e.g. 12, 16, 24, and 32), due to little or no magnetic fields in the OFF-state.

The design's performance deteriorates:

1. at increasing internal grasp diameters of the radial bellows (Fig. 9, marker colors), due to strong magnetic fields in the OFF-state as the overall MR fluid mass is located radially closer to the Halbach mechanism and its magnet segments. In addition,

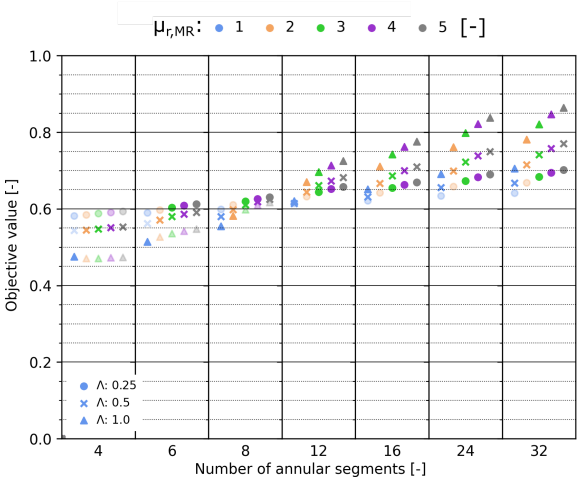

Figure 8: Multi-objective function's output for two concentric Halbach cylinders with dipoles as a function of the MR fluid's relative permeability $\mu_{r,MR}$ (marker colors), the number of annular segments n per cylinder, and the total area fraction ${}^1\Lambda$ (marker symbols). It is assumed that the radial bellows are fully inflated, which corresponds to an internal grasp diameter d_g of 10 mm. The relative magnetic permeability of the grasped object in the gripper's core $\mu_{r,obj}$ is set to 1.0. Even numbers of magnet segments were studied, with the spread per number of magnet segments for better visibility.

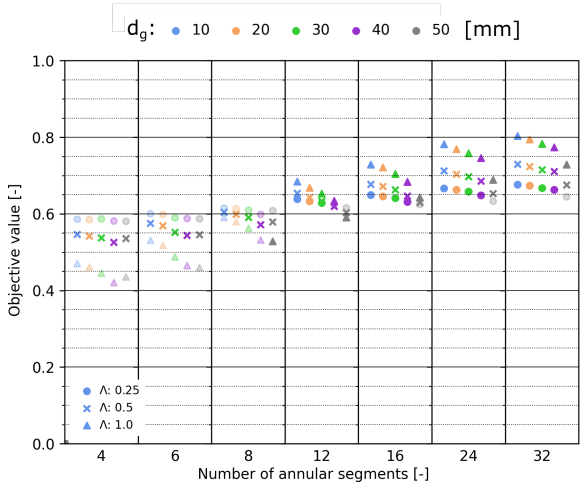

Figure 9: Multi-objective function's output for two concentric Halbach cylinders with dipoles as a function of the radial bellows' internal grasp diameter d_g [mm] (marker colors), the number of annular segments n per cylinder, and the total area fraction $^1\Lambda$ (marker symbols). The MR fluid's relative magnetic permeability is assumed to be a mean value of 2.5. The relative magnetic permeability of the grasped object in the gripper's core $\mu_{r,obj}$ is set to 1.0. Even numbers of magnet segments were studied, with the spread per number of magnet segments for better visibility.

the homogeneity of the magnetic fields in the ON-state also declines;

2. at increasing area fractions for small numbers of magnet segments (e.g. 4, 6, and 8), due to strong magnetic fields in the OFF-state. In general, larger area fractions are penalised because of the directly proportional relationship with the magnet areas and the declining field homogeneities. Additionally, the magnet area is independent of the MR fluid's relative permeability, the radial bellows' internal grasp diameter, and the number of annular magnet segments;
3. at small numbers of annular magnet segments (e.g. 4 and 6), the previously imposed constraints are not met with regard to the minimum and maximum magnetic flux densities in the radial bellows. In particular, small area fractions cannot generate minimum magnetic flux densities of 250 mT in the ON-state, while large area fractions cannot limit their magnetic flux densities to a maximum of 50 mT in the OFF-state (i.e. transparent data points).

5.2. *Halbach mechanisms with square segments*

The influence of the MR fluid's relative permeability $\mu_{r,MR}$, the radial bellows' internal grasp diameter d_g, the number of square segments n per cylinder, and the total area fraction $^1\Lambda$ on the performance of several concentric Halbach cylinder designs is examined (Fig. 10 - 11).

These designs differ from those with annular segments, as square magnets are fixed in annular cages. The magnet cages' relative permeabilities $\mu_{r,ca}$ are set to 1.0 (Fig. 7, gray area). This increases the affinity of the magnetic field lines to close through the more magnetically permeable MR fluid. For the other preconditions is referred to those for annular segments (sec. 5.1, preconditions: 1 to 6).

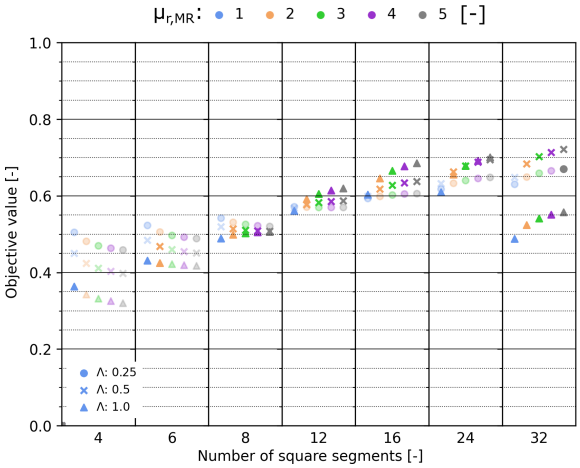

Figure 10: Multi-objective function's output for two concentric Halbach cylinders with dipoles as a function of the MR fluid's relative permeability $\mu_{r,MR}$ (marker colors), the number of square segments n per cylinder, and the total area fraction $^1\Lambda$ (marker symbols). It is assumed that the radial bellows are fully inflated, which corresponds to an internal grasp diameter d_g of 10 mm. The relative magnetic permeability of the magnet cage $\mu_{r,ca}$ and the grasped object in the gripper's core $\mu_{r,obj}$ is set to 1.0. Even numbers of magnet segments were studied, with the spread per number of magnet segments for better visibility.

The design's performance improves:

1. at increasing relative magnetic permeabilities of the MR fluid (Fig. 10, marker colors) for large numbers of magnet segments (e.g. 12, 16, 24, and 32). Because the mean magnetic flux densities in the OFF-state become insensitive for these increasing relative permeabilities, after a certain number of magnet segments. This makes the rising mean magnetic flux densities in the ON-state more decisive. Although of minor impact, the homogeneity of the magnetic fields in the ON-state declines;
2. at increasing numbers of square magnet segments, due to strongly decreasing mean magnetic flux densities in the OFF-state against increasing mean

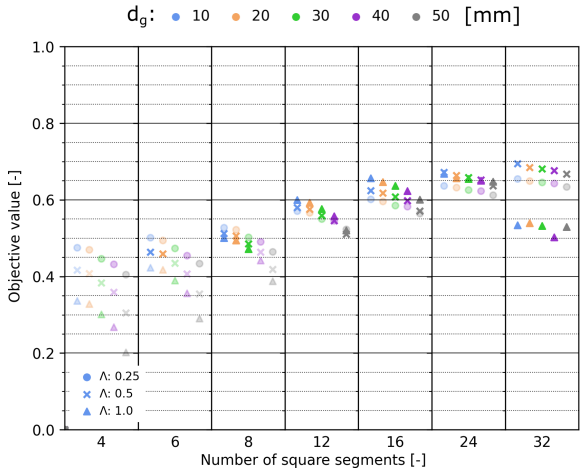

Figure 11: Multi-objective function's output for two concentric Halbach cylinders with dipoles as a function of the radial bellows' internal grasp diameter d_g [mm] (marker colors), the number of square segments n per cylinder, and the total area fraction $^1\Lambda$ (marker symbols). The MR fluid's relative magnetic permeability is assumed to be a mean value of 2.5. The relative magnetic permeability of the magnet cage $\mu_{r,ca}$ and the grasped object in the gripper's core $\mu_{r,obj}$ is set to 1.0. Even numbers of magnet segments were studied, with the spread per number of magnet segments for better visibility.

magnetic flux densities in the ON-state. In addition, the homogeneity of the magnetic fields in the ON-state also enhances, where even an overall better field homogeneity is observed compared to annular segments.

The design's performance deteriorates:

1. at increasing relative magnetic permeabilities of the MR fluid (Fig. 10, marker colors) for small numbers of magnet segments (e.g. 4, 6, and 8). Because of strong mean magnetic flux densities in the OFF-state for these increasing relative permeabilities;
2. at increasing internal grasp diameters of the radial bellows (Fig. 11, marker colors), due to strong magnetic fields in the OFF-state as the overall MR fluid mass is located radially closer to the Halbach mechanism and its magnet segments. In addition, the homogeneity of the magnetic fields in the ON-state also declines;
3. at increasing area fractions for small numbers of magnet segments (e.g. 4, 6, and 8), due to strong magnetic fields in the OFF-state. In general, larger area fractions are penalised because of the directly proportional relationship with the magnet areas and the declining field homogeneities. But, significantly large numbers of magnet segments (e.g. 24 and 32) are governed by low mean magnetic flux densities in the ON-state and large magnet areas, for both of which an optimum is found at 16 magnet segments. Besides this, the magnet area is independent of the MR fluid's relative permeability, and the radial bellows' internal grasp diameter;
4. at small numbers of magnet segments (e.g. 4, 6, and 8) and small area fractions (e.g. 0.25), the previously imposed constraints are not met with regard to the minimum and maximum magnetic flux densities in the radial bellows. In particular, small area fractions cannot generate minimum magnetic flux densities of 250 mT in the ON-state, while large area fractions cannot limit their magnetic flux densities to a maximum of 50 mT in the OFF-state (i.e. transparent data points).

6. Discussion

Based on the findings in Section 5, the following design guidelines for concentric Halbach mechanisms are drawn that recommend (in order to be applied in stiffness-adaptable robotic grippers):

1. a magnetic dipole, which prevails over a magnetic quadrupole, because of the lower mean magnetic flux density in the OFF-state and the more homogeneous magnetic field in the ON-state;
2. equally sized area fractions for both concentric cylinders, to get optimal field compensation in the Halbach mechanism's OFF-state;
3. a total area fraction between 0.5 and 1.0, to make a trade-off between a sufficiently powerful Halbach mechanism and a limited amount of magnetic material (i.e. high economic relevance);
4. a square magnet shape, since annular magnets are less commonly available and require special manufacturing, which increases the overall cost. However, in most related work [14, 27], annular segments are often employed as magnetic field sources;
5. a number of 16 magnet segments, which acts as an optimum in obtaining a compact Halbach mechanism (i.e. small magnet area) that can sufficiently stiffen the radial bellows' MR fluid (i.e. large mean magnetic flux density in the ON-state);
6. a mean relative magnetic permeability of 2.5 for MR fluid, which is reported by literature as a common value, as well as for ferrofluids [25, 26], that also corresponds to the authors' findings. An increased relative magnetic permeability is dominated by the chemical composition, weight percentage, and size of the magnetically permeable

Table 2: An optimised concentric Halbach cylinder design with a magnetic dipole, where the geometric parameters (i.e. GEOM.) are: n is the number of square segments, a is the magnet's side length [mm], r_i is the cylinder's inner radius [mm], r_o is the cylinder's outer radius [mm], ${}^2\Lambda$ is the area fraction per cylinder, ${}^1\Lambda$ is the total area fraction. The magnetic parameters (i.e. MAGN.) are: $\overline{B}_{ON}$ is the radial bellows' mean magnetic flux density in the ON-state [mT], $\overline{B}_{OFF}$ is the radial bellows' mean magnetic flux density in the OFF-state [mT], and ΔB_{ON} is the magnetic field's inhomogeneity in the ON-state (i.e. standard deviation) [mT].

GEOM.	n	a	r_i	r_o	${}^2\Lambda$	${}^1\Lambda$
Inner	16	10	38.0	56.7	0.35	0.83
Outer	16	15	56.7	84.5	0.35	

MAGN.	$\overline{B}_{ON}$	$\overline{B}_{OFF}$	ΔB_{ON}
Output	486	14.2	34.9

particles but which adversely affects the fluid's gravitational sedimentation stability, the magnetic field's homogeneity in the ON-state, and strength in the OFF-state;

7. a relative magnetic permeability of 1.0 (i.e. non-ferromagnetic) for the magnet cages, which increases the affinity of the magnetic field lines to close through the more magnetically permeable MR fluid. Ferromagnetic cages would act adversely as an internal yoke to the magnetic field;
8. a limited diameter of the object to be grasped, although of minor importance. In addition, non-ferromagnetic as well as ferromagnetic objects can be grasped, without major differences in performance. However, the latter could be positively influenced by the magnetic field's attraction in the gripper's core, resulting in an even more stable grasp.

The proposed design guidelines result in an optimised concentric Halbach cylinder design whose geometric and magnetic parameters are listed in Table 2. This Halbach mechanism has a multi-objective value of 0.649, and yields mean magnetic flux densities (i.e. ON: 486 mT; OFF: 14.2 mT) that amply meet the authors' flux constraints (i.e. ON: 250 mT; OFF: 50 mT) by a factor of 2 and 3.5, respectively. In addition, Fig. 12 shows the 2D field map in both operational states.

The purpose of this paper consisted in determining the influence of geometric and material parameters on the performance of two concentric Halbach cylinders, and drawing design guidelines to evolve towards an optimal Halbach mechanism for the magnetic activation of the proposed cylindrical radial bellow gripper filled with MR fluid. For this, a deliberate subset of the vast parameter space is explored using grid search. The design of (the most) optimal Halbach mechanism can be regarded as a multi-objective optimisation problem due to the significant number of parameters controlling the mechanism's performance. Because of the absence of a heuristic function, which steers the search process, uninformed search methods (e.g. grid search) are known to consume substantial amounts of time searching parts of the parameter space that will result in unfavourable designs.

Future research aims at (1) further expanding the search space by allowing to alter the number of magnet segments, the individual magnet sizes and orientations per cylinder; and (2) searching for the most optimal design in an automated fashion without any user intervention. Informed search techniques (e.g. Bayesian hyperparameter optimisation) will be studied that use the multi-objective function's output of previous runs to generate new promising sets of geometric and material parameters to explore, therewith converging significantly faster. In addition, two-dimensional magnetostatic analyses were performed therewith assuming an infinite cylinder length, and neglecting adverse side effects of field distortion at the end faces of the cylinders to which three-dimensional simulations may provide an answer [21, 28].

7. Conclusion

This study is part of the development of innovative hybrid gripper principles that possess the high compliance and degrees of freedom of soft grippers, enriched by the increased precision and grasping force of hard grippers. The proposed cylindrical radial bellow gripper is filled with magnetorheological (MR) fluid as a promising force-transferring medium, due to its controllable stiffness under an external magnetic field. This requires sufficiently strong, compact and adjustable magnetic field sources for which electromagnets are often regarded as the sole option available. However, permanent magnets possess higher magnetic flux densities per mass unit, and when assembled in certain ways, they even allow to control their joint magnetic field.

Finite element simulations are used to investigate the influence of geometric and material parameters on the performance of permanent magnet assemblies, in particular two concentric Halbach cylinders. These parameters include the magnets' shapes, sizes and number; the cylinders' radii and number of pole pairs; and the relative permeabilities of the MR fluid and the grasped

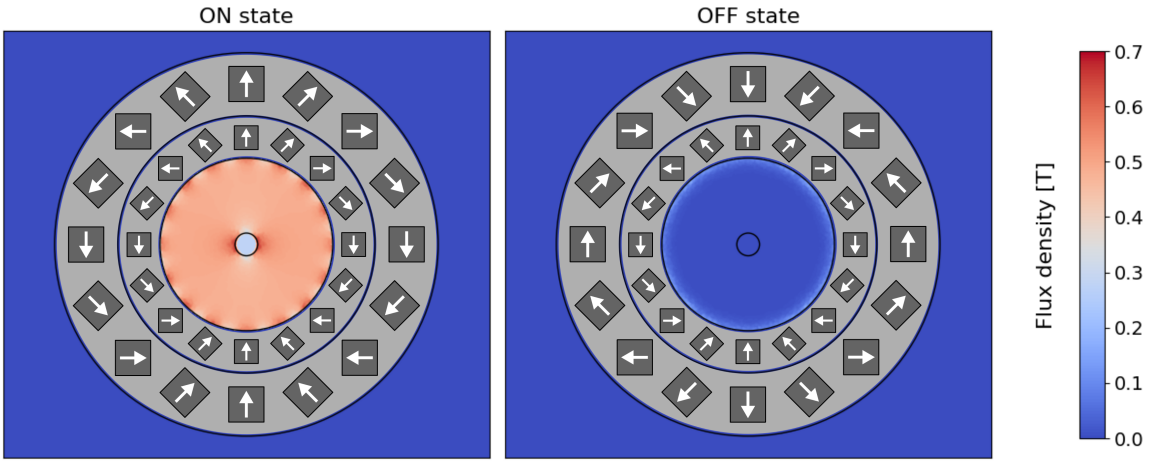

Figure 12: 2D field map demonstrating the magnetic flux densities in the ON (left) and OFF-state (right) of the optimal concentric Halbach mechanism (Table 2), for the proposed stiffness-adaptable robotic gripper, with an internal grasp diameter of 10 mm.

object. The performance of these Halbach mechanisms are measured by a normalized multi-objective function that considers: the mean magnetic flux densities generated in the mechanism's ON and OFF-state, the magnetic field's inhomogeneity (i.e. standard deviation) in the ON-state, and the total magnet area for both cylinders. Finally, guidelines are derived to evolve to an optimal Halbach mechanism in order to implement in the proposed MR-based gripper prototype.

8. Acknowledgements

Jeroen Cramer thanks KU Leuven, Diepenbeek Campus for granting a FLOF mandate therewith facilitating this research. Martijn Cramer is a SB PhD fellow at FWO (Research Foundation Flanders) under grant agreement 1SA6919N.

References

[1] J. Hughes, U. Culha, F. Giardina, F. Guenther, A. Rosendo, F. Iida, Soft manipulators and grippers: A review, Frontiers in Robotics and AI 3 (2016) 69. doi:10.3389/frobt.2016.00069.

[2] J. Shintake, V. Cacucciolo, D. Floreano, H. Shea, Soft robotic grippers, Advanced Materials 30 (29) (2018) 1707035. doi:10.1002/adma.201707035.

[3] J. R. Amend, E. Brown, N. Rodenberg, H. M. Jaeger, H. Lipson, A positive pressure universal gripper based on the jamming of granular material, IEEE Transactions on Robotics 28 (2) (2012) 341–350. doi:10.1109/TRO.2011.2171093.

[4] B. E. Schubert, D. Floreano, Variable stiffness material based on rigid low-melting-point-alloy microstructures embedded in soft poly(dimethylsiloxane) (PDMS), RSC Adv. 3 (2013) 24671–24679. doi:10.1039/C3RA44412K.

[5] A. Olabi, A. Grunwald, Design and application of magneto-rheological fluid, Materials & Design 28 (10) (2007) 2658–2664. doi:10.1016/j.matdes.2006.10.009.

[6] J. Cramer, M. Cramer, E. Demeester, K. Kellens, Exploring the potential of magnetorheology in robotic grippers, Procedia CIRP 76 (2018) 127–132, 7th CIRP Conference on Assembly Technologies and Systems (CATS 2018). doi:10.1016/j.procir.2018.01.038.

[7] K. Weiss, J. Carlson, A growing attraction to magnetic fluids, 1994.

[8] X. Zhu, X. Jing, L. Cheng, Magnetorheological fluid dampers: A review on structure design and analysis, Journal of Intelligent Material Systems and Structures 23 (8) (2012) 839–873. doi:10.1177/1045389X12436735.

[9] B. Shrestha, H. Hao, K. Bi, Devices for protecting bridge superstructure from pounding and unseating damages: an overview, Structure and Infrastructure Engineering 13 (3) (2017) 313–330. doi:10.1080/15732479.2016.1170155.

[10] Y. Li, J. Li, W. Li, H. Du, A state-of-the-art review on magnetorheological elastomer devices, Smart Materials and Structures 23 (12) (2014) 123001. doi:10.1088/0964-1726/23/12/123001.

[11] T. J. Kang, K. H. Hong, H. Jeong, Preparation and properties of a p-aramid fabric composite impregnated with a magnetorheological fluid for body armor applications, Polymer Engineering & Science 55 (4) (2015) 729–734. doi:10.1002/pen.23826.

[12] W. Kordonski, D. Golini, Multiple application of magnetorheological effect in high precision finishing, Journal of Intelligent Material Systems and Structures - J INTEL MAT SYST STRUCT 13 (2002) 401–404. doi:10.1106/104538902026104.

[13] H. Leupold, E. Potenziani, A. Tilak, Adjustable multi-tesla permanent magnet field sources, IEEE Transactions on Magnetics 29 (6) (1993) 2902–2904. doi:10.1109/20.281092.

[14] R. Bjørk, C. R. Bahl, A. Smith, N. Pryds, Comparison of adjustable permanent magnetic field sources, Journal of Magnetism and Magnetic Materials 322 (22) (2010) 3664–3671. doi:10.1016/j.jmmm.2010.07.022.

[15] R. Bjørk, A. Smith, C. Bahl, Analysis of the magnetic field, force, and torque for two-dimensional halbach cylinders, Journal of Magnetism and Magnetic Materials 322 (1) (2010) 133–141. doi:10.1016/j.jmmm.2009.08.044.

[16] S. Celik, M. H. Kural, Octagonal halbach magnet array design for a magnetic refrigerator, Heat Transfer Engineering 39 (4) (2018) 391–397. doi:10.1080/01457632.2017.1305846.

[17] E. Danieli, J. Mauler, J. Perlo, B. Blümich, F. Casanova, Mobile sensor for high resolution NMR spectroscopy and imaging, Journal of Magnetic Resonance 198 (1) (2009) 80–87. doi:10.1016/j.jmr.2009.01.022.

[18] P. Blümler, F. Casanova, Chapter 5 hardware developments: Halbach magnet arrays, in: Mobile NMR and MRI: Developments and Applications, The Royal Society of Chemistry, 2016, pp. 133–157. doi:10.1039/9781782628095-00133.

[19] O. Baun, P. Blümler, Permanent magnet system to guide superparamagnetic particles, Journal of Magnetism and Magnetic Materials 439 (2017) 294–304. doi:10.1016/j.jmmm.2017.05.001.

[20] R. Tao, Super-strong magnetorheological fluids, Journal of Physics: Condensed Matter 13 (50) (2001) R979–R999. doi:10.1088/0953-8984/13/50/202.

[21] R. Bjørk, The ideal dimensions of a Halbach cylinder of finite length, Journal of Applied Physics 109 (1) (2011). doi:10.1063/1.3525646.

[22] H. Raich, P. Blümler, Design and construction of a dipolar Halbach array with a homogeneous field from identical bar magnets: NMR mandhalas, Concepts in Magnetic Resonance Part B: Magnetic Resonance Engineering 23B (1) (2004) 16–25. doi:10.1002/cmr.b.20018.

[23] K. Halbach, Design of permanent multipole magnets with oriented rare earth cobalt material, Nuclear Instruments and Methods 169 (1) (1980) 1–10. doi:10.1016/0029-554X(80)90094-4.

[24] M. Ashtiani, S. Hashemabadi, A. Ghaffari, A review on the magnetorheological fluid preparation and stabilization, Journal of Magnetism and Magnetic Materials 374 (2015) 716–730. doi:10.1016/j.jmmm.2014.09.020.

[25] D. Mayer, P. Polcar, A novel approach to measurement of permeability of magnetic fluids, Przeglad Elektrotechniczny (2012).

[26] A. Zakinyan, Y. Dikansky, Drops deformation and magnetic permeability of a ferrofluid emulsion, Colloids and Surfaces A: Physicochemical and Engineering Aspects 380 (1) (2011) 314–318. doi:10.1016/j.colsurfa.2011.03.018.

[27] Q. Chen, G. Zhang, Y. Xu, X. Yang, Design and simulation of a multilayer Halbach magnet for NMR, Concepts in Magnetic Resonance Part B: Magnetic Resonance Engineering 45 (3) (2015) 134–141. doi:10.1002/cmr.b.21292.

[28] H. Soltner, P. Blümler, Dipolar Halbach magnet stacks made from identically shaped permanent magnets for magnetic resonance, Concepts in Magnetic Resonance Part A 36A (2010) 211 – 222. doi:10.1002/cmr.a.20165.